PARTITIONING OF NUCLEI IN CENTRAL $^{129}Xe + ^{nat}Sn$ COLLISIONS FROM 25 TO 50 A MeV.

R.Dayras[a,*], J.-L.Charvet[a], L.Nalpas[a], C.Volant[a],
(INDRA collaboration)
a) DAPNIA/SPhN, CEA/Saclay F-91191, Gif sur Yvette, Cedex, France
* Corresponding author, e-mail: rdayras@cea.fr

Abstract

Charge distributions measured in central $^{129}Xe + ^{nat}Sn$ collisions from 25 to 50 AMeV bombarding energy are analyzed in the framework of a random break-up model. Many aspects of the data stem from finite size effects. This simple approach based on integer number decomposition gives a remarkable description of the data for bombarding energies equal or greater than 39 AMeV. The implications of these results will be discussed.

1 INTRODUCTION

In this presentation, we examine the evolution of various observables linked to the charge distributions of the fragments produced in central $^{129}Xe + ^{nat}Sn$ collisions measured with INDRA from 25 to 50 A MeV bombarding energies. Previous analyses [1, 2] of charge correlations on these data suggested that spinodal decomposition may occur from 32 to 39 A MeV incident energy. However, a recent analysis [3] using a different technique did not confirm those results. Thus, we thought it was important to look at the evolution of the reaction mechanisms in the same energy range using a different approach. Here, we compare the experimental distributions to the ones computed from the partitions of nuclei of charge $Z_b = \sum_{i=1}^{i=M_{IMF}} Z_i$, where Z_i is the charge of fragment i and M is the number of fragments in an event. To avoid structure effects linked to very light fragments only fragments with $Z_i \geq 5$ are considered. Similar approaches have been undertaken in the past [4-6] in order to reproduce inclusive charge and mass distributions in high energy collisions. It was assumed there that all partitions had the same probability. In our case, we assume that each partition is weighted by the number of different possible realization of that partition. In the next section we will recall few relations on the partitioning of integers.

2 PARTITIONING OF INTEGERS

In this section we remind few formulae on the partitioning of integers. Considering an integer Z_b, the number of different ways this integer can be decomposed into M integers is given by

$$N_M(Z_b) = \binom{Z_b - 1}{M - 1} = \frac{(Z_b - 1)!}{(M - 1)!(Z_b - M)!} \quad (1)$$

Note that $N_M(Z_b)$ is not the number of partitions as computed in refs. [5, 6] but it takes into account all the different ways of realizing the same partition. Thus each partition, i, has a weight given by,

$$P_i(Z_b|M) = \frac{M!}{\prod_{z_i} n_{z_i}!} \quad (2)$$

where n_{z_i} is the number of times the number z_i appears in the partition. Irrespectively of the multiplicity M, the total number of ways of decomposing the integer Z_b is given by,

$$N(Z_b) = \sum_{M=1}^{Z_b} N_M(Z_b) = 2^{Z_b - 1} \quad (3)$$

For a given multiplicity M, the size distribution is given by the relation,

$$P_M(Z) = M \times \binom{Z_b - Z - 1}{M - 2} \quad (4)$$

Now, if we decompose the number Z_b into integers greater or equal to a minimum value Z_m, the above relations can be generalized. Thus, relation (1) becomes:

$$N_M^{Z_m}(Z_b) = \begin{pmatrix} Z_b - M \times (Z_m - 1) - 1 \\ M - 1 \end{pmatrix} \quad (5)$$

whereas the size distribution for a multiplicity M is given by the following relation,

$$P_M^{Z_m}(Z) = M \times \begin{pmatrix} Z_b - (M-1)Z_m - Z + M - 2 \\ M - 2 \end{pmatrix} \quad (6)$$

We note that this way of partitioning an integer into *M* parts is equivalent to break *M*-1 bounds at random in a chain containing Z_b nodes and keeping only configurations in which all fragments contain at least Z_m nodes.

In the experimental data, for each event, the multiplicity M_{IMF} is defined as the number of fragments with $Z \geq Z_m = 5$. In an event, the charge bound into fragments is defined as $Z_b = \sum_{i=1}^{M_{IMF}} Z_i$. For each value of the multiplicity M_{IMF}, the corresponding Z_b distribution is built. Then, for this multiplicity, the charge distribution is calculated according to the relation,

$$P_M(Z) = \sum_{Z_b} w(Z_b) \times P_M^{Z_m}(Z) \quad (7)$$

where $P_M^{Z_m}(Z)$ is given by the relation (6) and $w(Z_b)$ is a weighting factor for a proper normalization to the data,

$$w(Z_b) = \frac{N_M^{ex}(Z_b)}{N_M^{Z_m}(Z_b)} \quad (8)$$

in which $N_M^{ex}(Z_b)$ is the number of events with a value Z_b and $N_M^{Z_m}(Z_b)$ is given by relation (5).

In order to make more detailed comparisons with experimental data, for a given multiplicity M_{IMF}, starting from the Z_b distribution, we compute for each value of Z_b all ordered partitions which are considered as events. For a proper normalization, each partition is given the weight $w(Z_b)$ defined by relation (8). These partitions, are then treated as experimental events.

3 COMPARISONS TO DATA

3.1 Data selection

Only events for which the total detected charge was greater or equals to 80, as compared to 104,
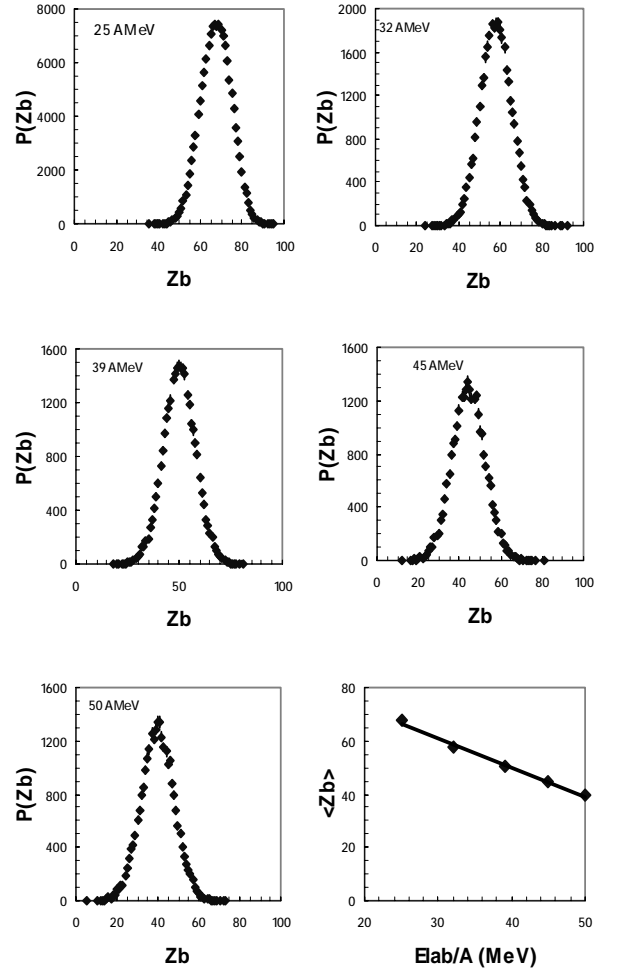
Figure 1: Evolution of the experimental Z_b distributions as a function of bombarding energy, from 25 to 50 AMeV, for central *Xe + Sn* collisions. The error bars are statistical only. Bottom right, average $<Z_b>$ as a function of the bombarding energy. The straight line is a linear fit to the data.

the total charge of the *Xe + Sn* system were retained. In order to select the most central collisions, as in previous analyses [1-3] a complementary selection was made taking only events with a flow angle greater than 60°. For this purpose, the kinetic energy tensor was built using all fragments with $Z \geq 3$. It has been shown [7, 8)] that such events can be associated to the multifragmentation of a compact source.

For this selection, the average multiplicity $<M_{IMF}>$ of fragments with $Z \geq 5$ increases first with bombarding energy from 3.7±1.0 at 25 AMeV to reach a maximum of 4.9±1.3 at 39 AMeV then decreases to 4.4±1.2 at 50 AMeV
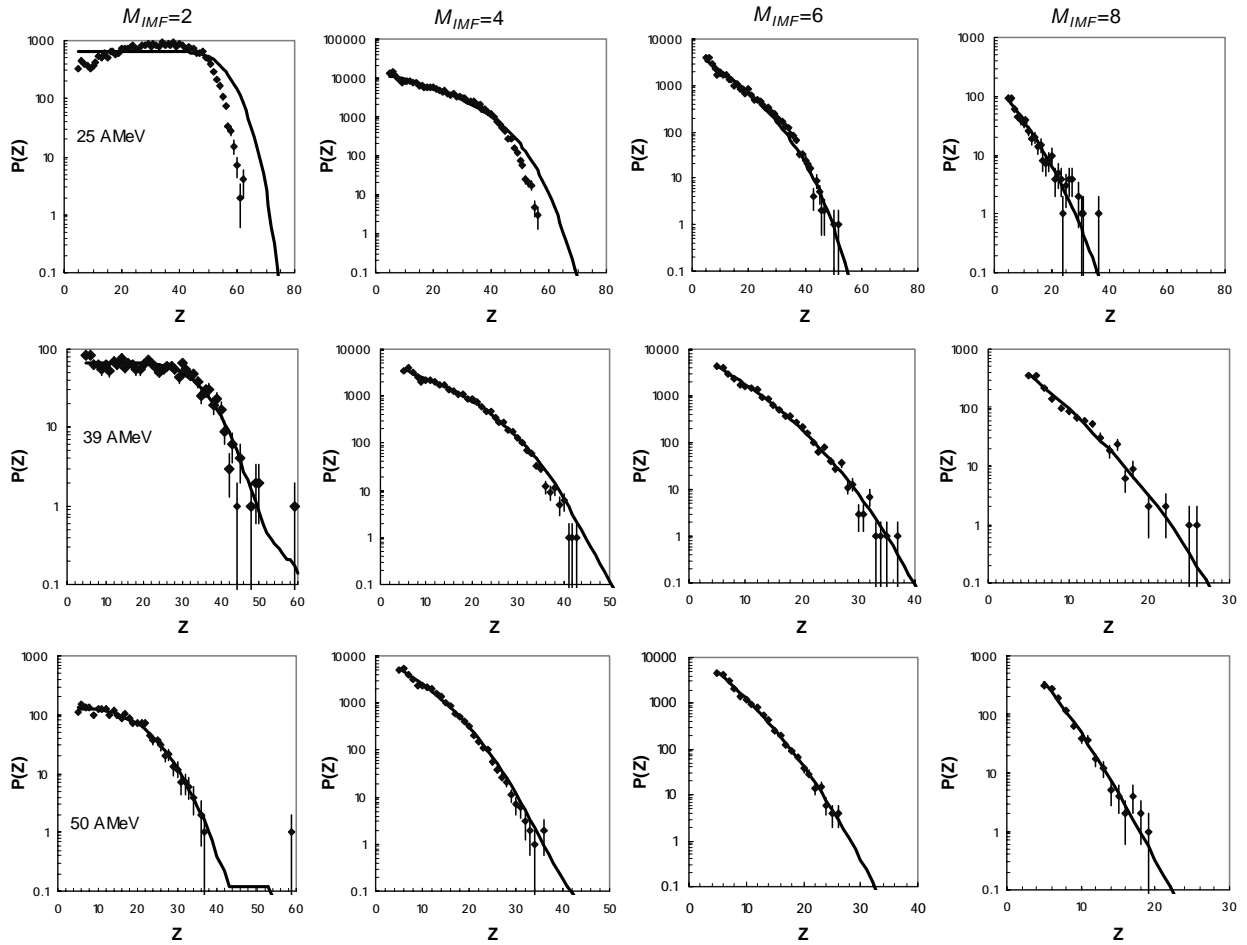
Figure 2: From top to bottom, charge distributions for central $^{129}Xe + {}^{nat}Sn$ collisions at 25, 39 and 50 AMeV bombarding energies for fragment multiplicities $M_{IMF} = 2$, 4, 6 and 8, from left to right. The error bars on the experimental data are statistical only. The full drawn curves are calculated using relation (7).

(the quoted errors are in fact the standard deviations of the multiplicity distributions). The evolution of the Z_b distributions as a function of bombarding energies is shown in fig. 1. These distributions are Gaussians with a mean value which decreases linearly, at a rate of one charge unit per MeV/nucleon, with bombarding energies as shown by the bottom right panel of fig. 1. This behavior is expected from charge conservation as more and more light fragments and particle are produced when the bombarding energy increases.

At each bombarding energy, the Z_b distributions were built for each fragment multiplicity M_{IMF}. These distributions are also of gaussian shape with mean values which increase almost linearly with M_{IMF}. The rate of increase is 3.13 charge units per IMF at 25 AMeV and reaches 4.4 charge units per IMF at 50 AMeV. These

distributions are then used to compute the ordered partitions of nuclei of charge Z_b as described above. In the next section, we compare the charge distributions thus calculated to the experimental ones.

3.2 Charge distributions

Experimental charge distributions are presented in figure 2 for three bombarding energies, 25, 39 and 50 AMeV (rows), for four values of the IMF multiplicity, $M_{IMF} = 2$, 4, 6 and 8 (columns). The charge distributions calculated using relation (7), are shown by the full drawn curves. From 39 AMeV to 50 AMeV bombarding energies, the experimental data are quite well reproduced by relation (7), even for binary break-up. When the energy is lowered, discrepancies start to appear for the lowest IMF multiplicities, $M_{IMF} \leq 4$ at 32 AMeV and $M_{IMF} \leq 5$ at

25 AMeV. In those cases, the calculated distributions extend to larger charges than the experimental ones. By examining in details the Z distributions of the biggest, the second biggest and so on fragments for each IMF multiplicities, it was found out that these discrepancies came mainly from the calculated Z distributions of the biggest fragment. Indeed, it was found that the calculated distributions of these fragments extend to larger Z values than the experimental ones whereas the Z distributions of the lighter fragments are correctly reproduced.

In the following section, we investigate the standard deviations of the charge distributions.

3.3 Charge correlations

Following Moretto *et al*. [9], the average IMF charge in an event is defined as $<Z> = \dfrac{1}{M_{IMF}} \sum\limits_{i=1}^{M_{IMF}} Z_i$ and the standard deviation

for that event is given by,

$$\Delta Z = \sqrt{\sum_{i=1}^{M_{IMF}} (Z_i - <Z>)^2 / (M_{IMF} - 1)} \; .$$

The experimental distributions P(ΔZ) are shown for the three bombarding energy, 25, 39 and 50 AMeV, in the three rows of figure 3 for four different values of the IMF multiplicity (columns). The strong oscillations observed for $M_{IMF} = 2$ are numerical effects due to the integer nature of the charges. The distributions calculated from the ordered partitions are shown by the full drawn curves in figure 3. For the partitioning of an infinite system, it can be shown that $P(\Delta Z) \propto \Delta Z^{M_{IMF}-2}$. Thus, for such a system, $P(\Delta Z)$ should be flat for $M_{IMF} = 2$ and tends to infinity for larger values of M_{IMF}. The fall-off of $P(\Delta Z)$ is essentially a finite size effect. The position of the maximum depends upon the size of
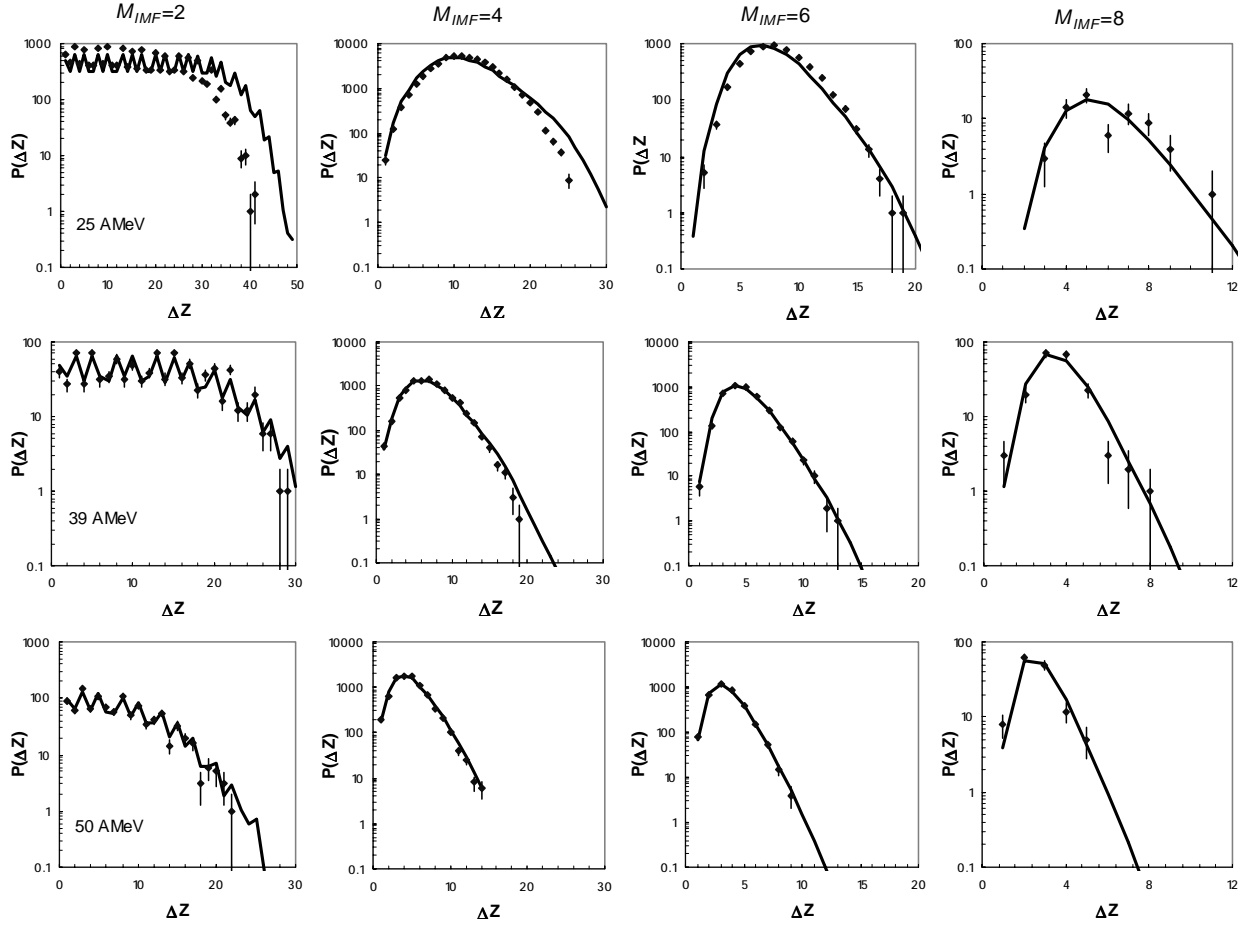

Figure 3: From top to bottom, ΔZ distributions for central $^{129}Xe + ^{nat}Sn$ collisions at 25, 39 and 50 AMeV bombarding energies for fragment multiplicities $M_{IMF} = 2$, 4, 6 and 8, from left to right. The error bars on the experimental data are statistical only. The full drawn curves are calculated from the ordered partitions (see text).

the fragmenting system, moving up as the size of the system increases. As Z_b decreases with the bombarding energy (figure 1) the maximum of the $P(\Delta Z)$ distribution moves to lower values of ΔZ. We note that for low ΔZ values (below the maximum), the ΔZ distributions follows closely the power law $P(\Delta Z) \propto \Delta Z^{M_{IMF}-2}$. There again, for bombarding energies equal to or greater than 39 AMeV, the ordered partitions yield a good agreement with the experimental data. For lower energies and low IMF multiplicities, as already mentioned the calculated distributions are too broad.

An excess production of nearly equal size fragments is predicted in different scenarios of nuclear multifragmentation [10-18] The ratio between the experimental and calculated ΔZ distributions can be considered as the charge correlation function defined by Moretto *et al.* [9]. As it was already observed in ref. [3], no particular enhancement in the first ΔZ bin is observed in the data over the calculation (see figure 3). Thus, the present analysis rather suggests a random break-up of the nuclei, more in line with the predictions of ref. [19].

3.4 Scaling law.

By inspecting relations (5) and (6), one notes that by replacing Z_b by $Z_b' = Z_b - M_{IMF} \times (Z_m - 1)$, one recovers relations (1) and (4) in which there is no restriction on the minimum size of the fragments ($Z_m = 1$). Thus, all previous could be obtained from relations (1) to (4) and the unrestricted ordered partitions of Z'_b in which $(Z_m - 1) = 4$ is added to the charge of each fragments. In figure 4a is given the evolution of $\langle Z_b \rangle$ as a function of bombarding energy for the various IMF multiplicities. From 25 to 50 AMeV bombarding energies, $\langle Z_b \rangle$ spans 20 to 30 charge units when the IMF multiplicity increases from 2 to 9. Figure 4b gives the same evolution for $\langle Z'_b \rangle$. All values of $\langle Z'_b \rangle$ collapse in narrow band (less than 4 charge units wide) whatever the multiplicity is. This suggests that at each bombarding energy, a Z'_b distribution may exist, which is independent of the IMF multiplicity. This is indeed the case as shown by figure 4c in
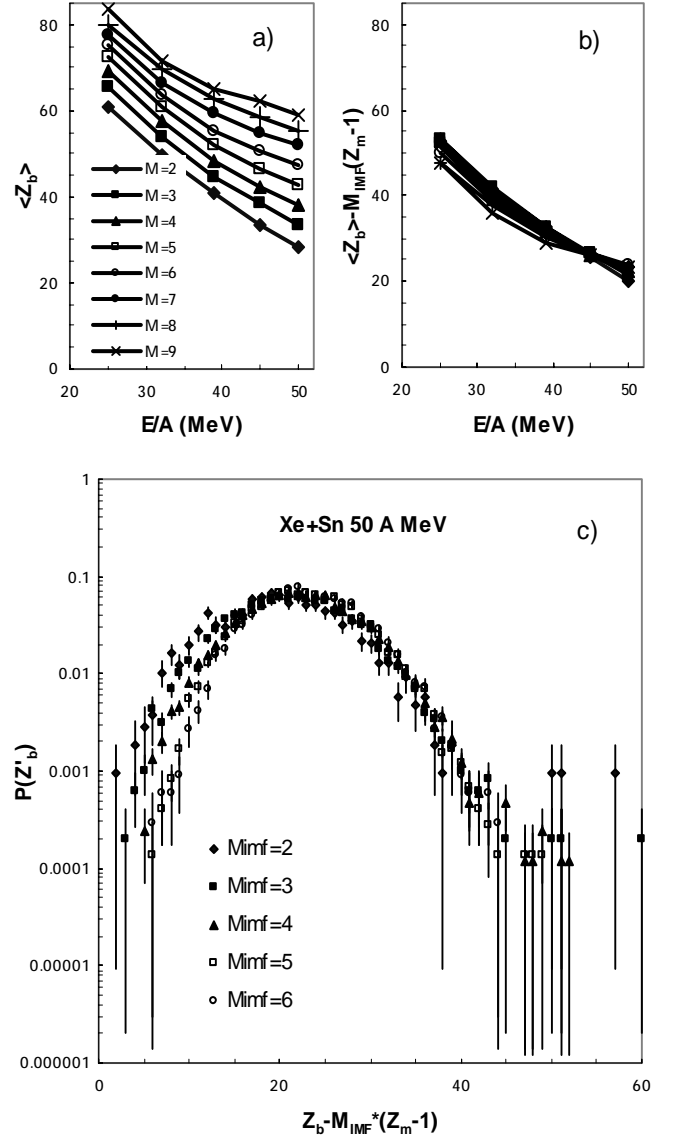
Figure 4: a) Dependence of $\langle Z_b \rangle$ upon the incident energy as a function of the IMF multiplicity. b) Same as a) by replacing $\langle Z_b \rangle$ by $\langle Z_b \rangle - 4 \times M_{IMF}$. All the data points in a narrow band less than 4 charge units wide. The lines are just to guide the eye. c) After substituting $Z'_b = Z_b - 4 \times M_{IMF}$ to Z_b, the Z'_b distributions normalized to unity superimpose. The error bars on the data points are statistical only.

which all Z'_b distributions are superimposed whatever the IMF multiplicity at 50 AMeV bombarding energy. For the sake of comparison all distributions have been normalized to unity. The superimposition is quite good for $Z'_b > 15$ whereas there is some dispersion for the lower values of Z'_b. The same type of agreement is obtained down to 32 AMeV bombarding energy

whereas at 25 AMeV only the distributions for $M_{IMF} \geq 5$ superimpose correctly.

4 DISCUSSION AND SUMMARY.

Multifragmentation in central $^{129}Xe +^{nat}Sn$ collisions have been analysed in the framework of a random break-up of the multifragmenting source. Neglecting secondary decay, it is assumed that the fragmenting nuclei belong to the experimental Z_b distributions where for each event $Z_b = \sum_{i=1}^{M_{IMF}} Z_i$ with $Z_i \geq 5$. At a given bombarding energy, the Z_b distributions depend upon the IMF multiplicity as shown figure 4a. However, this observation does not necessary means that events with different IMF multiplicities are produced by sources of different size but more likely results from the competition with light fragment and particle emission. For the present analysis the events belonging to different IMF multiplicity are treated separately. One of the essential features of the present analysis is to take into account properly final size effects.

For bombarding energies greater or equal to 39 AMeV, whatever the IMF multiplicity, starting from the Z_b distributions, the partitions of the system can be fully described assuming a random break-up. As the incident energy is lowered, this description starts to fail for the lowest IMF multiplicities. At the lowest measured energy (25 AMeV), only events with $M_{IMF} \geq 5$ are properly described. In those cases, the size of the biggest fragment predicted by a random break-up is too large whereas the size of the other fragments is still estimated correctly.

One plausible explanation of the evolution observed with bombarding energy is that above 39 AMeV incident energy, the excitation energy of the system is such that all partitions become likely. When the incident energy is lowered the partitions consuming the largest amount of energy become unfavourable. This will happen first for low IMF multiplicity events in which a large amount of light fragments and particles are produced, consuming a large amount of the available energy.

An alternative interpretation is to assume that above 39 AMeV bombarding energy the system enters a completely disordered phase. Frankland *et al.* [20], using a model independent universal fluctuation theory, have also analysed central *Xe + Sn* collisions. They observe a change of Δ-scaling of the largest fragment in each event, from $\Delta \sim 0.5$ below 39 AMeV bombarding energy to $\Delta \sim 1$ above. This change may also signal the transition from an ordered to a disordered phase.

The scaling law observed between the Z_b distributions suggests that it may be possible to find a unique distribution permitting a unified description of the data at a given bombarding energy.

5 REFERENCES

[1] B.Borderie et al., INDRA Collaboration, Phy. Rev. Lett. 86(2001)3252.

[2] G.Tabăcăru et al., Eur. Phys. J. A18(2003)103.

[3] J.-L.Charvet et al., Nuclear Physics A730(2004)431.

[4] J.Aichelin and J.Huefner, Phys. Lett. 136B(1984)15.

[5] J.Aichelin et al., Phy. Rev. C30(1984)107.

[6] L.G.Sobotka and L.G.Moretto, Phys. Rev. C31(1985)668.

[5] P.Désesquelles, Phy. Rev. C65(2002)034603.

[6] P.Désesquelles, Phy. Rev. C65(2002)034604.

[7] N.Marie et al., Phy. Lett. B391(1997)15.

[8] J.D.Frankland et al., INDRA Collaboration, Nucl. Phys. A689(2001)905.

[9] L.G.Moretto et al., Phys. Rev. Lett. 77(1996)2634.

[10] G.Bertsch and P.Siemens, Phys. Lett. B126(1983)9.

[11] S.Ayik, M.Colonna and Ph.Chomaz, Phys. Lett. B353(1995)417.

[12] Ph.Chomaz et al., Phys. Rev. Lett. 73(1994)3512.

[13] B.Jacquot et al., Phys. Lett. B383(1996)247.

[14] A.Guarnera et al., Phys. Lett. B403(1997)191.

[15] L.G.Moretto et al., Phys. Rev. Lett. 69(1992)1884.

[16] W.Bauer, G.F.Bertsch and H.Schulz, Phys. Rev. Lett. 69(1992)1884.

[17] H.M.Xu et al., Phys. Rev. C48(1993)933.

[18] L.G.Moretto et al., Phys. Rev. Lett. 77(1996)2634.

[19] D.Lacroix, A.Van Lauwe and D.Durand, this conference and to be published in Phys. Rev. C.

[20] J.D.Frankland et al., INDRA Collaboration, this conference.